

Photonic Enabled RF Self-interference Cancellation for Full-duplex Communication

Xiyou Han^{1*}, Xinxin Su¹, Shuo Wang¹, Hanqiao Wang¹, Yuchen Shao¹, Chao Wang², and Mingshan Zhao¹

¹School of Optoelectronic Engineering and Instrumentation Science, Dalian University of Technology, Dalian, 116024, China

²School of Engineering and Digital Arts University of Kent Canterbury, CT2 7NT, U.K.

*E-mail address: email: xyhan@dlut.edu.cn

Abstract: A photonic approach based on phase modulation and optical sideband filtering for cancelling the RF self-interference in full-duplex communication system is proposed and experimentally demonstrated with good cancellation performance.

OCIS codes: (060.2330) Fiber optics communications; (120.5060) Phase modulation; (130.7408) Wavelength filtering devices;

1. Introduction

Compared with the time division duplex and the frequency division duplex, the full duplex operation transmits and receives simultaneously in the same frequency band, which improves the spectral efficiency and enhances the throughput greatly. Therefore the full-duplex technique has broad applications in the fifth generation (5G) wireless communication and new satellite communication [1]. It has attracted more and more attention not only in academic community but also in industry [2]. However, due to the collocation of the transmitting and receiving antennas in the full-duplex system, the high power transmitted signal will interfere with the in-band weak received signal, which is known as RF self-interference. The conventional methods, such as notch filters or narrow bandpass filters cannot resolve this problem because the same frequency band is used for both transmitter and receiver. In the past few years electronic self-interference cancellation (SIC) methods including the RF cancellation and digital cancellation have been developed to remove the RF self-interference [3]. However, these methods always suffer from narrow bandwidth and low precision time delay

To overcome the limitations in electronic SIC systems, we propose and demonstrate experimentally a novel approach for photonic RF SIC by using phase modulation and optical sideband filtering. In the photonic SIC system, the left sideband of the received RF phase-modulated signal and the right sideband of tapped RF phase-modulated signal are filtered out by a single optical filter. Due to the inherent out-of-phase property between the right and left sidebands of the filtered phase-modulated signals, the RF SIC is realized during the O/E conversion upon the PD by tuning the amplitude and delay time of the phase-modulated signal in the optical domain. Compared with the previous Mach-Zehnder modulator (MZM) based schemes [5]-[6], this approach avoids the complicated DC bias voltage control devices. It also has the capability for operating on the higher frequency range and wider bandwidth, compared with the direct modulation schemes [7]-[9]. The operation principle of the proposed scheme is analyzed and the feasibility is demonstrated experimentally.

2. System structure and operation principle

The schematic of the proposed optical RF SIC system is shown in Fig. 1. Two lasers with different wavelengths of λ_1 and λ_2 are sent to two phase modulators PM_1 and PM_2 , respectively. The received RF signal $s(t)+i(t)$ from the receiver antenna, where $s(t)$ is signal of interest and $i(t)$ is interference signal, is modulated on the light wave of λ_1 via PM_1 . The tapped RF signal $r(t)$ from the transmitter (Tx), as the reference signal, is modulated on the light wave of λ_2 via PM_2 . Through a VOA and a TODL, the phase-modulated signal in the lower path is combined with the phase-modulated signal in the upper path via a 3dB optical coupler (OC) and fed to an optical filter (OF). After being filtered by the OF, the optical signals are input to the photo detector (PD).

Due to the inherent property of phase modulation, the left and right sidebands of phase-modulated signal are out of phase as shown the spectra at point A and B in Fig. 1. The phase-modulated optical signals in the upper path and the lower path before the OF can be expressed as

$$E_{upper} = E_1 e^{\left[j2\pi f_{c1}t + j \frac{V_i \cos(2\pi f_{RF}t)}{V_{\pi 1}} \right]} \quad (1)$$

$$E_{lower} = E_2 \sqrt{\alpha} e^{\left[j2\pi f_{c2}(t'+\tau) + j \frac{V_r \cos[2\pi f_{RF}(t'+\tau)]}{V_{\pi 2}} \right]} \quad (2)$$

where E_1 , E_2 , f_{c1} and f_{c2} are the amplitude and frequency of the light waves from the two lasers; α is the power attenuation coefficient of the VOA; τ is the delay time of the TODL; $V_{\pi 1}$ and $V_{\pi 2}$ are the half-wave voltage of PM₁ and PM₂, respectively; V_i and V_r are the amplitude of the interference signal and reference signal; f_{RF} is the frequency of the RF signal. For simplicity, the signal of interest is not included in Eq. (1), which doesn't affect the validity of the deduction. By using the Jacobi–Anger expansions, Eqs. (1) and (2) can be expressed as

$$E_{upper} = E_1 \left\{ J_1(m_1) e^{j2\pi(f_{c1}-f_{RF})t} + J_0(m_1) e^{j2\pi f_{c1}t} + J_1(m_1) e^{j[2\pi(f_{c1}+f_{RF})t+\pi]} \right\} \quad (3)$$

$$E_{lower} = E_2 \sqrt{\alpha} \left\{ J_1(m_2) e^{j2\pi(f_{c2}-f_{RF})(t'+\tau)} + J_0(m_2) e^{j2\pi f_{c2}(t'+\tau)} + J_1(m_2) e^{j[2\pi(f_{c2}+f_{RF})(t'+\tau)+\pi]} \right\} \quad (4)$$

where J_0 , J_1 are the 0 and 1st-order Bessel function of the first kind. When deriving Eq. (3) and (4), only the 0- and ± 1 st-order components are considered. The left sideband of the received RF modulated optical signal in the upper path and the right sideband of the tapped RF modulated optical signal in the lower path are filtered out by the OF. As shown the spectrum at point C in Fig. 1, the single sideband with carrier (SSB+C) optical signals are obtained and can be expressed as

$$E_{upper} = E_1 \left\{ J_0(m_1) e^{j2\pi f_{c1}t} + J_1(m_1) e^{j[2\pi(f_{c1}+f_{RF})t+\pi]} \right\} \quad (5)$$

$$E_{lower} = E_2 \sqrt{\alpha} \left\{ J_1(m_2) e^{j2\pi(f_{c2}-f_{RF})(t'+\tau)} + J_0(m_2) e^{j2\pi f_{c2}(t'+\tau)} \right\} \quad (6)$$

The RF signals are recovered by the O/E conversion from the SSB+C optical signals upon the PD, and can be expressed as

$$I_{ac1} \propto ac \left(\rho \cdot E_{upper} \cdot E_{upper}^* \right) = A_1 \cos(2\pi f_{RF}t + \pi) \quad (7)$$

$$I_{ac2} \propto ac \left(\rho \cdot E_{lower} \cdot E_{lower}^* \right) = A_2 \cos[2\pi f_{RF}(t' + \tau)] \quad (8)$$

where $A_1 = 2\rho E_1^2 J_0(m_1) J_1(m_1)$, $A_2 = 2\rho \alpha E_2^2 J_0(m_2) J_1(m_2)$, ρ is the responsivity of the PD.

As can be seen from Eqs. (7) and (8), when $A_1 = A_2$, $t = t' + \tau$ are realized by properly tuning the power attenuation coefficient α of the VOA and the time delay τ of the TODL, the recovered reference signal I_{ac2} cancels the recovered interference signal I_{ac1} . The signal of interest is therefore obtained

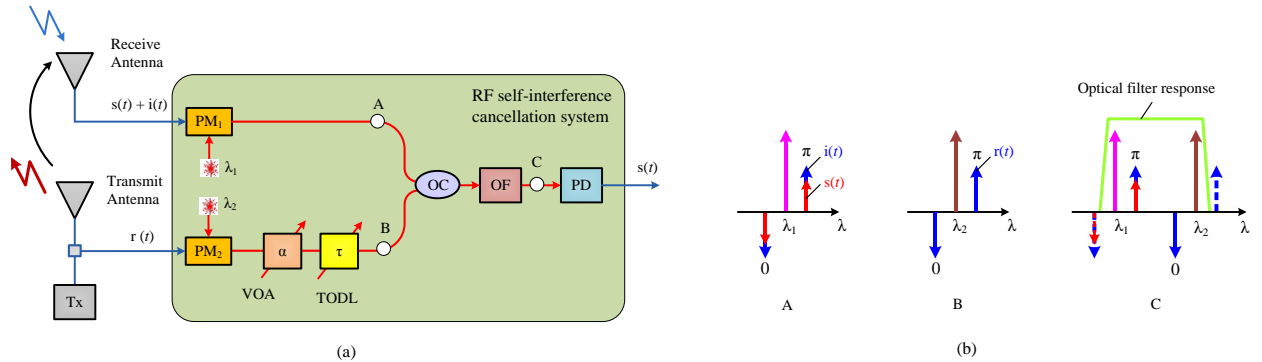


Figure 1. (a) The structure of the proposed optical RF SIC system. (b) The spectra of the phase-modulated optical signals before (A and B) and after (C) the OF. PM, phase modulator; VOA, variable optical attenuator; TODL, tunable optical delay line; OC, optical coupler; OF, optical filter; PD, photodetector; Tx, transmitter.

3. Experimental results and analysis

With the established experimental setup, the feasibility of the proposed photonic RF SIC approach is demonstrated. The RF signal from a signal generator (SG1, Agilent E8257D) is used as the signal of interest $s(t)$. The RF signal from a second signal generator (SG2, Agilent E8267D) is split to two parts by an electronic 3dB splitter. One part is input to PM₂ as the reference signal $r(t)$ and the other part is used as the interference signal $i(t)$. Figure 2(a) and 2(b) show the optical spectra of the phase-modulated signals ($f_{RF}=10$ GHz) before and after the optical filter (OF), respectively. It can be seen that the single sideband with carrier (SSB+C) signals have been

achieved by the OF. Therefore, the RF signals can be recovered by the O/E conversion from the SSB+C optical signals upon the PD.

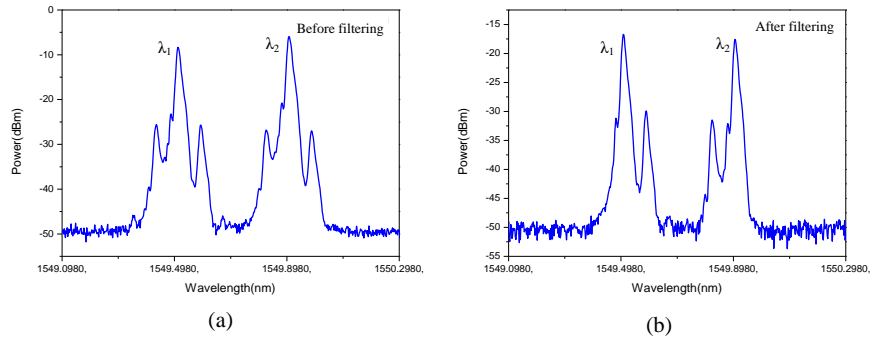


Figure 2. The optical spectra of the phase-modulated signals (a) before and (b) after the optical filter

In order to investigate the cancellation performance for RF signal with a certain bandwidth, the arbitrary (ARB) signal with a bandwidth of 20 MHz is modulated on the RF signal from SG2. A 10 GHz single tone signal with a power of -40 dBm from SG1 is used as the signal of interest. With the laser source of λ_2 being turned off, a strong interference signal is observed in the electrical spectrum as shown the red/dash curve in Figure 3(a). Then, by tuning on the laser source of λ_2 , the 20 MHz bandwidth interference signal is suppressed greatly with a cancellation depth as high as 34 dB and the desired 10 GHz signal is maintained, as shown the blue/solid curve in Figure 3(a). The cancellation performance for bandwidth of 50 MHz and 100 MHz are also investigated and the results are shown in Figure 3(b) and 3(c), with cancellation depth of 30 dB and 25 dB, respectively, illustrating the capability of the RF SIC for wider bandwidth.

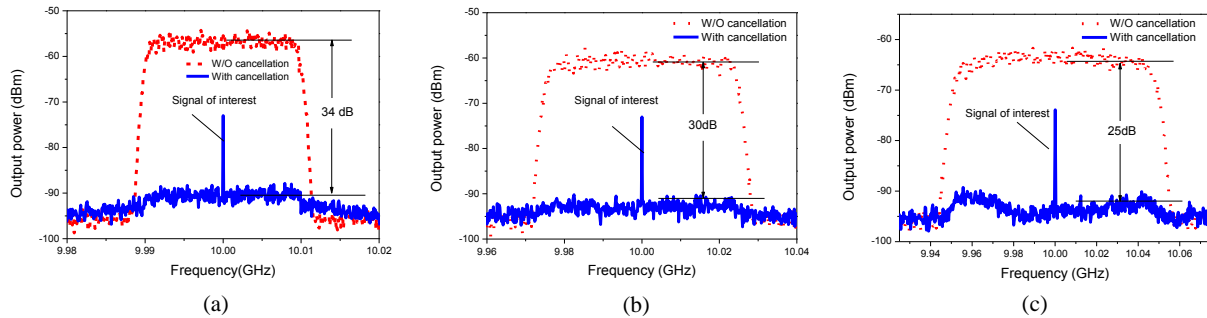


Figure 3. The output RF spectra of an interference signal bandwidth of (a) 20MHz, (b) 50MHz and (c) 100 MHz with and without cancellation.

Acknowledgements

This work was supported in part by National Pre-Research Foundation of China (6140450010305), and Fundamental Research Funds for the Central Universities (DUT18ZD106, DUT18GF102, and DUT18LAB20).

4. References

- [1] A. Sabharwal, P. Schniter, D. Guo, et al. "In-band full-duplex wireless: challenges and opportunities," *IEEE J. Sel. Areas Comm.* 32(9): 1637–1652(2014).
- [2] Z.S. Zhang, X.M. Chai, K.P. Long, et al. "Full duplex techniques for 5G networks: self-interference cancellation, protocol design, and relay selection," *IEEE Communications Magazine*, 53(5): 128-137(2015).
- [3] S.K. Sharma, T.E. Bogale, L.B. Le, et al, "Dynamic spectrum sharing in 5G wireless networks with full-duplex technology: recent advances and research challenges," *IEEE Communications Surveys & Tutorials*, 20(1): 674-707(2018).
- [4] V.J. Urick, D.C. Mikeska, and M.E. Godinez, "Photonics for electronic interference suppression," *Avionics and Vehicle Fiber-Optics and Photonics Conference 2017 (AVFOP)*, New Orleans, Louisiana USA, 7-9 Nov. 2017. pp. 1-2.
- [5] Y. Zhang, S. Xiao, H. Feng, et al. "Self-interference cancellation using dual-drive Mach-Zehnder modulator for in-band full-duplex radio-over-fiber system," *Opt. Express*, 23(26): 33205–33213(2015).
- [6] X.Y. Han, B. Huo, Y. Shao, et al. "Optical RF self-interference cancellation by using an integrated dual-parallel MZM," *IEEE Photonics J.*, 9(2): 5501308(2017).
- [7] Q. Zhou, H.L. Feng, G. Scott, et al. "Wideband co-site interference cancellation based on hybrid electrical and optical techniques," *Opt. Lett.* 39(22): 6537-6540(2014).
- [8] M.P. Chang, E.C. Blow, M.Z. Lu, et al. "RF characterization of an integrated microwave photonic circuit for self-interference cancellation," *IEEE Trans. Microw. Theory Techn.*, 66(1): 596-605(2018).
- [9] J.J. Sun, M.P. Chang, and P.R. Prucnal, "Demonstration of over-the-air RF self-interference cancellation using an optical system," *IEEE Photon. Technol. Lett.*, 29(4): 397-400(2017).